Chemistry, Physics and Technology of Surface. 2024. V. 15. N 4. P. 534-551

UDC 543.54 + 544.72 + 544.726 + 544.35 + 546.831 + 66.081.6 doi: 10.15407/hftp15.04.534

Yu.S. Dzyazko [1], L.M. Rozhdestvenska [1], K.O. Kudelko [1], L.M. Ponomaryova [2], L.Ya. Shteinberg [3], T.V. Yatsenko [1]

POLYMER-INORGANIC MEMBRANES FOR REMOVAL OF PESTICIDES FROM WATER USING PRESSURE-DRIVEN TECHNIQUE

[1] V.I. Vernadskii Institute of General and Inorganic Chemistry of National Academy of Sciences of Ukraine
32/34 Academician Palladin Ave., Kyiv, 03142, Ukraine, E-mail: dzyazko@gmail.com
[2] Sumy State University
116 Kharkivska Str., Sumy, 40000, Ukraine
[3] Scientific and Technical Institution "Institute of Chemical Technology and Industrial Ecology"
3 Chemist's Sq, Rubizhne, 93000, Ukraine

Pesticides enter surface and ground waters not only from agricultural lands, but also from the plants, where these substances are produced and packed. Thus, the problem of wastewaters produced by these plants must be solved. This work is devoted to the development of high performance membranes for pressure-driven processes, which would remove pesticides from water and give a possibility to use the concentrate further. Polyamide (PA) and polyvinylidene fluoride (PVDF) microfiltration membranes as well as polyacrylonitrile (PAN) ultrafiltration membrane were modified with hydrated zirconium dioxide (HZD) by a deposition of ion exchanger from sol with ammonia vapour directly in pores of the polymer. The membranes were investigated with SEM method, energy dispersive and FTIR spectra were also recorded. HZD in active layer as well as the products of PA or PAN hydrolysis enhance hydrophilicity of the membrane surface: for instance, the contact angle of water decreases from 69° to 43° for the PA sample. Water test followed by calculation using the Hagen-Poiseuille equation showed a 2–3 times decrease in pore size of the modified membranes comparing with pristine materials. Selectivity of HZD-containing membranes reaches 90–96 % towards bowine serum albumin, and exceeds 99 % in the case of quizalofop-p-ethyl. The highest permeate flux (196 l m^{-2} $h^{-1}$$bar^{-1}$) has been found for the HZD-containing PVDF sample. The pesticide concentration in the permeate was 0.0002–0.008 mg l^{-1}. The posttreatment of the permeate involved adsorption on biochar under dynamic conditions. The method of liquid chromatography showed that after the passage through the column, no pesticide was detected in the permeate or its content was lower than maximal allowable concentration for surface water (0.0001 mg l^{-1}).

***Keywords**: ultrafiltration, microfiltration, pesticide, hydrated zirconium dioxide, adsorption*

INTRODUCTION

Due to fast economical activity in a global scale, a wide nomenclature of new water pollutant enters the environment [1, 2]. Surface water and ground water are defenceless against synthetic chemical substances, which are containing in industrial, agricultural and municipal wastes [3]. Each year, about 0.5 trillion tons of dangerous organic compounds are discharged to natural reservoirs, particularly water supply sources [4]. It should be stressed that liquid wastes contain small amounts of many hazardous compounds, a maximal allowable concentration of which is too low. Thus, a problem of the protection of environment and human health against risky organic substances is extremely important.

Pesticides, which involve insecticides, herbicides and fungicides, occupy a special position among dangerous organic compounds, since many of them are soluble in water or form stable emulsions or suspensions [5]. Due to a huge area of agricultural grounds, practically each source of water supplier (especially small streams [6]) is available for these compounds. Pesticides are also widely used in households as well as in parks, stadiums and other urban green spaces [7, 8]. Their transport to aquatic environment depends on the weather, soils, behaviour of pesticide and their application techniques [9–11].

Other sources of pesticides are the plants, when they are produced and packaged, and also container processing plants [12–14]. In this case, pesticides appear in ground and surface water

through sewage. Other way is evaporation from opened platforms. Then these substances enter surface water with atmospheric precipitations [15, 16]. The results are loss of biodiversibility caused by a penetration of the pesticides to food chains due to their transmission through direct contact, ingestion, or inhalation [17, 18]. The pesticide toxicity affects on physiology, growth, immunity, reproduction, hemato-biochemical profile of fishes, these substances provoke histopathological alterations of tissues of aquatic organisms [19]. Undegraded compounds can enter human bodies via drinking water [20, 21] as well as via aquatic flora and fauna, which are used as food [22, 23]. Regarding human health, the action of pesticides can be divided to short-term (headaches, eye and skin irritation, nausea, dizziness) and long-term (asthma, diabetes and cancer) [24, 25]. Due to this fact, the problem of removal pesticides from wastes is very important. That is why a number of strategies (chemical, physical and biological) of water decontamination has been developed [26].

Chemical removal of pesticides involves ozonation [27], photocatalytic degradation [28] and oxidation [29] as well as their combination, for instance, photocatalytic ozonation [30, 31] or photo-Fenton reactions [32]. The methods must provide full degradation of these compounds down to CO_2 and H_2O without formation of hazardous by-products [33–35]. It is a purpose of oxidation, but it cannot always be achieved [36]. Regarding the plants producing and packing pesticides, full degradation means a loss of these valuable substances.

The same disadvantages are attributed to electrochemical and biological methods – nevertheless, they are widespread. Electro-chemical treatment, particularly electro-Fenton process [32], involves radical generation via electrochemical reactions, which cause the pesticide destruction [37, 38]. The strategy of anodic oxidation – cathodic precipitation has been proposed in [39]: phosphorus-containing pesticide was oxidized and deposited in a form of hydroxylapatite. Electrooxidation was combined with electrodialysis [40] and electrocoagulation [41]. In the last case, the first stage of pesticide removal is their concentration by electrocoagulation, the second stage is electrooxidation or electro-Fenton process [42]. However, electrocoagulation can be used without the assistance of other electrochemical methods [43]. Despite high efficiency and fast degradation, these techniques require unfavourable operation cost additionally to the abovementioned disadvantages [44]. Capacitive electrodeionization is much attractive from the economical point of view, however, it is suitable for a small volume of water [45].

Both microorganisms [46–48] and enzymes extracted from them [49] are also applied to pesticide degradation – biological method is less expensive comparing with chemical and electrochemical oxidation. Activated sludge [50] or enzymes [51] are combined with photocatalysis. It should be noted that microorganisms and enzymes are sensitive to pH and temperature (besides their capability to destroy valuable products) [52].

A common approach to the removal of pesticides from water is adsorption. A number of adsorbents are used: from conventional (granular activated carbon [53], biochar obtained with chemical [54] or hydrothermal [55] techniques, clay minerals [56], synthetic mesoporous silica materials, particularly zeolites [57], chitosan-based materials [58]) to advanced substances (graphene [59] and its composite [60], metal [61] and covalent [62] organic frameworks). However, the regeneration of adsorbents is accompanied by the pesticides degradation. Moreover, adsorption is suitable for the removal of small amounts of substances. This disadvantage is also attributed to such membrane process as membrane distillation [63].

Baromembrane separation, such as nanofiltration [64], reverse [65] and forward osmosis [66] can be applied to the pesticide recovery from rather concentrated solutions. In these cases, the concentrate solution can be used repeatedly. However, nanofiltration and reverse osmosis require high pressure, the problems of forward osmosis is a slow rate of this process and treatment of the draw solution.

To overcome these problems, microfiltration and ultrafiltration are proposed in this work. Earlier this approach was used for the treatment of tea infusions [67], wastewater [68] and wines [69]. The membrane selectivity did not exceed 80 % [67] or 60–70 % [69]. Higher selectivity was suggested in [68], but in this case the membrane was modified with a ferment, which provided the pesticide degradation. But it is known that membrane modifying with inorganic

ion exchangers enhance their rejection ability [70–72]. Moreover, these modifiers hydrophilize membranes providing their stability against fouling with organic substances. In this case, the inorganic modifiers act similarly to a widespread hydrophilizing agent as graphene oxide, which is used for modifying polymer [72–74] and inorganic [75, 76] membranes.

The aim of this work is to develop membranes, which would able to reject pesticides without their destruction under low pressure on the one hand and possess stability against fouling with organic substances on the other hand. Ultra- and microfiltration membranes made of different polymers were investigated. Hydrated zirconium dioxide (HZD) was chosen as a modifier, since its precipitation allows one to obtain the smallest particles among hydrated oxides of multivalent metals [77]. Thus, HZD can be deposited in the active layer of membranes protecting them against fouling and enhancing their separation ability. The tasks of the work involved (i) modifying polymer membranes, (ii) study of their morphology and hydrophilicity, (iii) testing towards water, calibrating solution and pesticide solution, (iv) posttreatment of the permeate solution.

EXPERIMENTAL

Modifying and characterization of membranes. Materials produced by SuezSepa company (Sterlitech, USA) were applied to investigations. We used microfiltration composite membrane based on polyester macroporous support, an active layer was prepared from polyamide (Fig. 1) similarly to [78]. The membrane thickness was 0.1 mm. This composite material was marked as PA. Other microfiltration membrane, a thickness of which was 0.2 mm, was made of polyvinylidene fluoride (PVDF). At last, ultrafiltration membrane (0.055 mm of a thickness) consisting of non-woven lavsan (support) and polyacrylonitrile (active layer) was studied. This membrane was marked as PAN.

Sol for the membrane treatment was prepared from $ZrOCl_2$ salt similarly to [60, 79]. Membranes were degassed in water using a vacuum pump, immersed in sol containing 0.1 M Zr. Then they were put into a dessicator over a 0.1 M NH_4OH solution. As expected, this approach (the retardation of precipitation) would provide a formation of aggregated particles, which completely fill the membrane pores. The fluid transport was assumed to be realized through the pores between the primary particles in the aggregates. As mentioned in [79], a size of the primary particles is 6 nm. It should be noted that HZD is used for modifying proton conducting membranes [80] although this ion exchanger cannot provide high concentration of free charge carrier, since the pH of the point of zero charge is about 7 [81] (however, it can be shifted to acidic region by combining HZD with oxide of other multivalent metal [82, 83]). This modifier keeps high proton conductivity of the membranes under elevated temperatures due to water bonded with functional (hydroxide) groups [80]. It means, HZD could hydrophilize nonconductive membranes for pressure-driven separation.

After HZD precipitation, the membranes were rinsed with deionized water, dried under ambient conditions down to constant mass, treated in a Bandelin ultrasonic bath (Bandelin, Hungary) at 30 kHz, and dried again. Polymer-inorganic samples were marked as PA-HZD, PVDF-HZD and PAN-HZD.

Morphology and chemical composition of the PAN samples were studied by means of a Tescan Mira 3LMU scanning electron microscope with an In Beam detector (TESCAN, Czech Republic). In order to investigate PI membranes, a JSM-6060 LA microscope (JEOL, Japan) was used. A SEO-SEM Inspect S50-B microscope was applied to study PVDF samples. Preliminarily membranes were coated with an ultrathin layer of gold (PAN), platinum (PI) or silver (PVDF). In order to determine the total amount of HZD (in a form of dehydrated ZrO_2), a weighted sample was combusted at 1000 °C.

Membrane wetting with water was investigated with a Attension Theta Lite Tensiometer (Biolin Scientific, USA). The FTIR spectra of the active layer of pristine membranes were recorded with a Spectrum BX FT-IR spectrometer (PerkinElmer Instruments, USA). Preliminarily the active layer was separated from the macroporous substrate. A part of the polymer was treated with a HCl solution, the pH of which corresponded to that of Zr-containing sol. Then the samples were grinded in liquid nitrogen and compressed with KBr.

Water test. Tangential plate-and-frame module was applied to investigations, the effective area of membrane was 16 cm^2

(2 cm×8 cm). Filtration was carried out at 20 °C, the pressure was kept at the level of 0.5–2 bar. Cumulative volume (V) of the liquid at the outlet of the membrane module was recorded under predetermined time (τ). Non-linear regions of the $V-\tau$ curves corresponded to the membrane compression, linear regions are attributed to steady state. Water flux through the membrane (J_w) was calculated from the slopes of steady state regions [84]:

$$J_w = \frac{dV}{d\tau}\frac{1}{A}. \quad (1)$$

Here A is the effective membrane area.

Filtration of solutions. Membranes were calibrated using a solution of bowine serum albumin (BSA), molecular mass of which is 69 kDa. Filtration was carried out at 1 bar, a concentration of the feeding solution was 59 mg l^{-1}, its volume was 0.5 l. The solution was analyzed with a Bradford method involving Coomassie brilliant blue G-250 [85]. The velocity of the feeding solution was ≈ 100 cm^3 min^{-1}.

As a model object, a Queen Star Max herbicide produced by Ukravit (Ukraine) was used for investigations. The active substance of this pesticide is quizalofop-p-ethyl (QPE, see Fig. 1), its initial concentration was 59 g l^{-1}. The preparation was diluted in 1000 times with tap water, the feeding solution containing 59 mg l^{-1} was obtained by this manner. Filtration was performed at 0.5–2 bar and 20 C (PA-HZD) and 1 bar (other membranes). The samples of solution were taken and analyzed further using an Agilent 1290 liquid chromatograph supplied with an Agilent 6400 triple quadrupole detector (Agilent, USA).

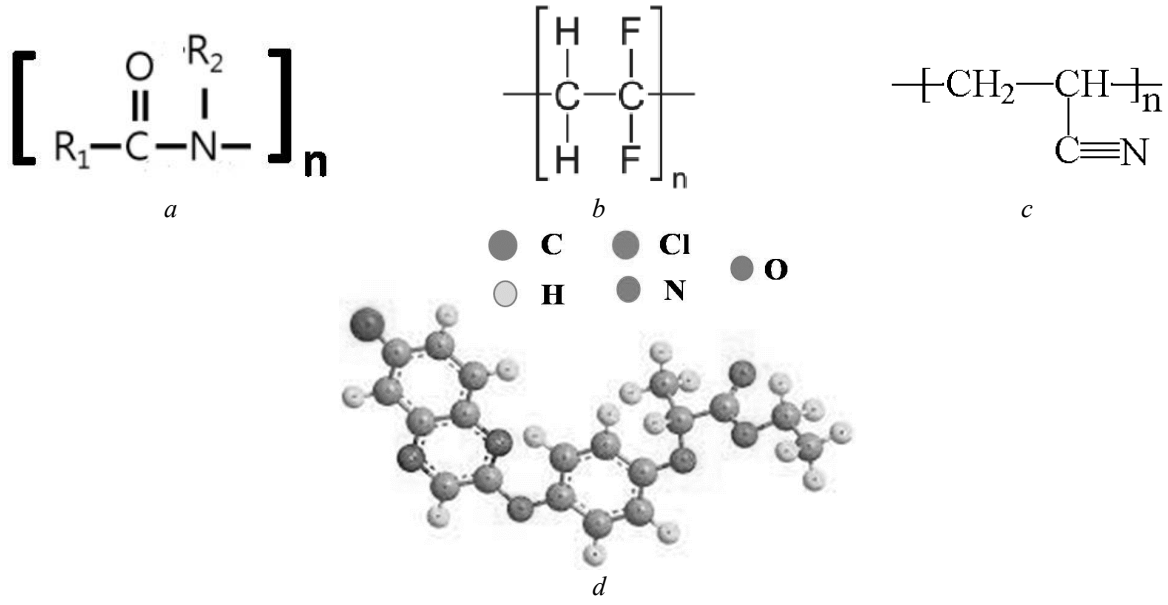

a *b* *c* *d*

Fig. 1. Polyamide (*a*), polyvinylidene fluoride (*b*), polyacrylonitrile (*c*) and quizalofop-p-ethyl, QPE (*d*)

Selectivity of the membranes (φ) was determined via:

$$\phi = \left(1 - \frac{C}{C_0}\right) \times 100\%, \quad (2)$$

where C and C_0 are the concentrations of permeate and feeding solution respectively. In order to estimate the membranes fouling, such parameter as flux decline ratio (FDR) [86] was used:

$$FDR = \left(1 - \frac{J}{J_w}\right) \times 100\%, \quad (3)$$

where J is the permeate flux. The smaller this parameter, the less fouling.

Postreatment of permeate. Residual QPE amount was removed with biochar, a method of the synthesis of this material was reported in [54]. Briefly: lactose ("Agrocapital of Ukraine" LTD Company, Ukraine) was mixed with two volumes of concentrated H_2SO_4 under cooling,

the mixture was activated with ultrasound, heated at 120 C under periodic ultrasonic activation, washed with deionized water up to pH 7 of the effluent.

The permeate passed through the column: its diameter was 0.8 cm, the bed volume was 5 cm^3. The solution velocity was 0.15 $cm^3\ s^{-1}$. Probes of the effluent were taken regularly and analyzed with a chromatographic method.

RESULTS AND DISCUSSION

Composition and morphology of membranes. Typical SEM images of pristine and modified micro- and ultrafiltration membranes are given in Fig. 2. In the case of PA microfiltration membrane, the size of pores of the active layer is 100–500 nm. The shape of the pores is mainly irregular or close to round. The pores are either at a considerable distance from each other, however, the distance between them is less than 100 nm. Comparing with the pristine membrane, the surface of modified material is more relief, the size of holes decreases down to 50–300 nm.

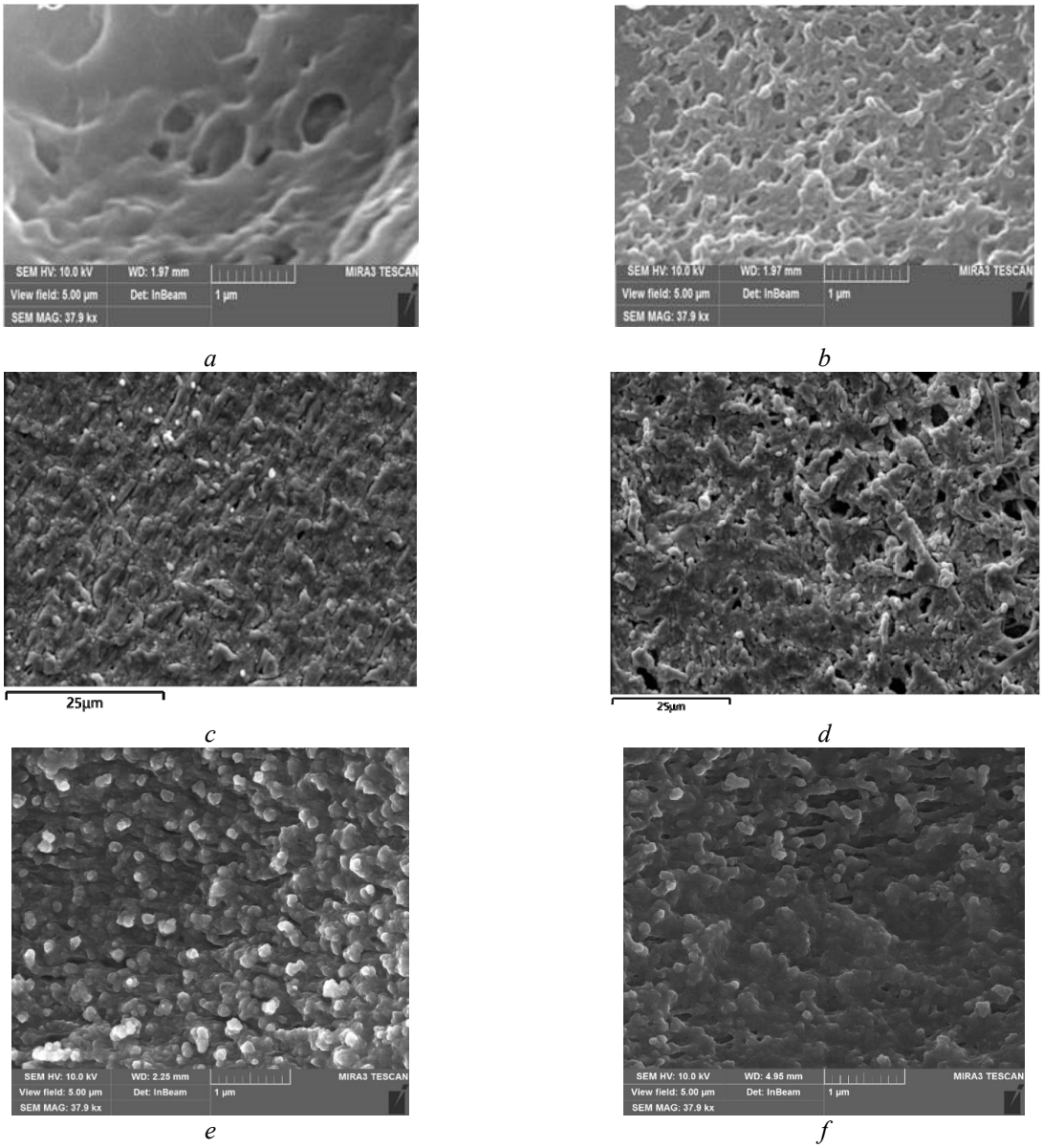

Fig. 2. SEM images of PA (*a*, *b*), PVDF (*c*, *d*) and PAN samples. Membranes: pristine (*a*, *c*, *e*) and modified (*b*, *d*, *f*)

Unlike PA samples, the PVDF membrane shows a widening of pores after modifying (up to several microns). At the same time, the pristine material shows much smaller holes (approximately several hundred nanometers). Regarding the PAN samples, blocks of polymer are visible on the surface, narrow slit-like pores are seen between them. Some blocks stuck together after modifying, the holes become wider.

Chemical analysis showed the highest HZD content on the surface of PAN membranes (Fig. 3, Table 1). Trace amount of Cl was also found, this element is originated from $ZrOCl_2$ salt, which was used for sol preparation. At the same time, much smaller Zr content is located just under the active layer. No Zr was found in the macroporous support: the particles of inorganic ion-exchanger is evidently located irregularly making them difficult to detect. It should be noted that the elemental analysis shows both C and N elements on the surface of active layer. It means HZD is between the polymer regions (cracks on the surface is caused by destructing action of electron beam during SEM observation). Since it is impossible to remove HZD from the surface with ultrasound, it means strong fixation of this inorganic ion exchanger. It is possible due to acidic or alkaline hydrolysis of PAN, which is caused by acidic sol and NH_3 vapour respectively. A final stage of the hydrolysis is the formation of carboxyl groups:

$$R–C\equiv N+HCl+2H_2O\rightarrow R–COOH+NH_4Cl, \quad (4)$$

$$R–C\equiv N+NH_4OH+H_2O \rightarrow R –COONH_4+NH_3. \quad (5)$$

Hydrolysis is accompanied by the formation of copolymer consisting of acrylamide, acrylonitrile [87] or ammonium acrylate [88] units. Simultaneous HZD precipitation and polymer transformation cause strong fixation of the particles of inorganic ion exchanger.

Polyamide demonstrates similar behaviour in acidic and alkaline media: partial destruction leads to the formation of $–R_1$-COOH and R_2NH_2 fragments [89]. This transformation can also cause strong fixation of the modifier particles on the surface. Indeed, energy dispersive X-ray spectrum of the PA-HZD shows a presence of Zr on the outer surface of the membrane (Fig. 4). The modifier particles are surrounded with polymer, since carbon and nitrogen were also detected. Hydrolytic transformation of the polymer is confirmed by the data of FTIR spectroscopy (Fig. 5). The vibrations of CH_2 fragments and CH_3 end groups are expressed as stripes at 2950 (ν_s), 2850 (ν_{as}) and 1440 (δ) cm^{-1}, an intensive band at 1440 cm^{-1}corresponds to scissoring vibration of methylene groups in $–CH_2–CO–$ fragments [90]. Amide groups give a wide band at the region of > 3000 cm^{-1}, carbonyl groups are recognized from the band at 1720 cm^{-1}. The band at 1350 cm^{-1} can be attributed to the end CH_3 groups. Hydrolysis causes an increase of the intensity of the bands in a high frequency region due to OH fragments of carbonyl groups. The band at 1350 cm^{-1} becomes more intensive probably as a result of overlapping with the band of OH groups.

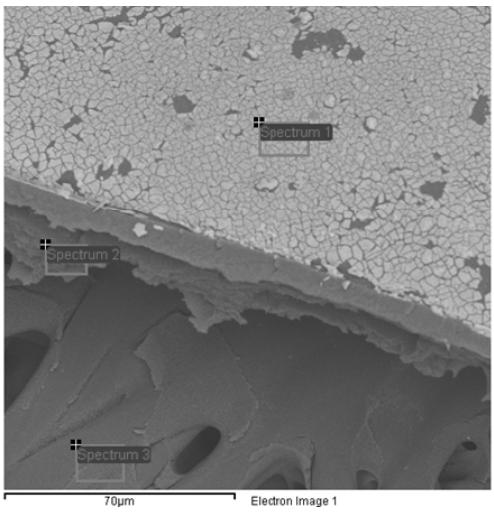

Fig. 3. Distribution of Zr through PAN-HZD membranes

Table 1. Chemical analysis of PAN-HZD membrane

Spectrum	Amount of element, atom. %					
	C	N	O	Cl	Zr	Total
Spectrum 1	37.36	3.32	32.08	0.79	26.46	100.00
Spectrum 2	60.01	23.73	15.17		1.09	100.00
Spectrum 3	62.08	9.62	28.30			100.00

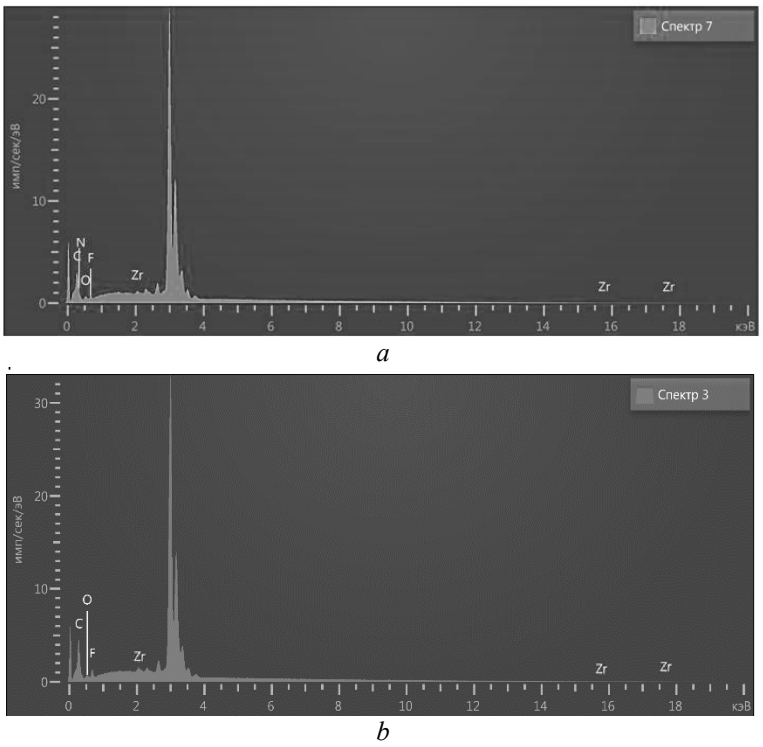

Fig. 4. Energy dispersive spectra for PA-HZD (*a*) and PVDF-HZD (*b*) samples. The most intensive peak corresponds to the coating material (Ag)

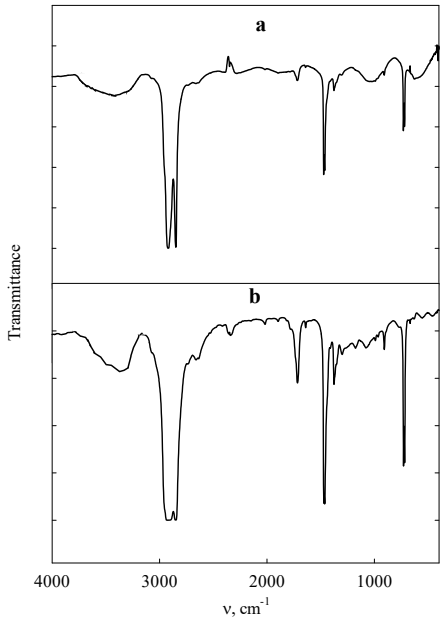

Fig. 5. FTIR spectra of pristine (*a*) and hydrolysed (*b*) polyamide

Elemental analysis showed a presence of Zr on the surface of chemically inert PVDF-based sample despite its preliminarily treatment with ultrasound (see Fig. 4). In general, the HZD content (determined as ZrO_2 after the burning membrane) increases within the order: PA-HZD < PAN-HZD < PVDF-HZD (Table 2): the thickest membrane shows the highest modifier content. It should be noted that acidic or alkaline hydrolysis of polyamide [91, 92] and polyacrylonitrile [93] filtration membranes enhances their hydrophilicity and improves their filtration performance.

Table 2. Modifier content in the membranes, their hydrophilicity and filtration performance

Membrane	Liquid	PA	PA-HZD	PVDF	PVDF-HZD	PAN	PAN-HZD
ZrO_2 content, mass %	–	–	3.5	–	15	–	4.1
Wetting angle, degree	Water	69.52	42.74	91.88	76.54	72.65	64.83
R, m^{-1}		1.23×10^{12}	3.71×10^{12}	3.82×10^{11}	6.39×10^{11}	2.02×10^{13}	1.26×10^{14}
ε		0.48	0.44	0.37	0.31	0.48	0.44
L, $l\ m^{-2}\ h^{-1}bar^{-1}$		324	108	1080	612	20	3
d, nm		103	62	305	80	19	8
FDR, %	BSA	87	81	93	89	64	44
L, $l\ m^{-2}\ h^{-1}bar^{-1}$		25	21	90	68	7	2
φ, %		0	90	0	96	97	98
FDR, %	Pesticide	97	75	98	65	92	37
L, $l\ m^{-2}\ h^{-1}bar^{-1}$		12	27	22.5	196	1.6	1.9
J, $m^3m^{-2}s^{-1}$		2.76×10^{-6}	7.5×10^{-6}	6.25×10^{-6}	6.11×10^{-5}	4.37×10^{-7}	5.28×10^{-7}
V/V_f		5	11	10	70	4	7
Residual concentration, mg l^{-3}		0.001	0.0003	0.008	0.005	0.0008	0.0002

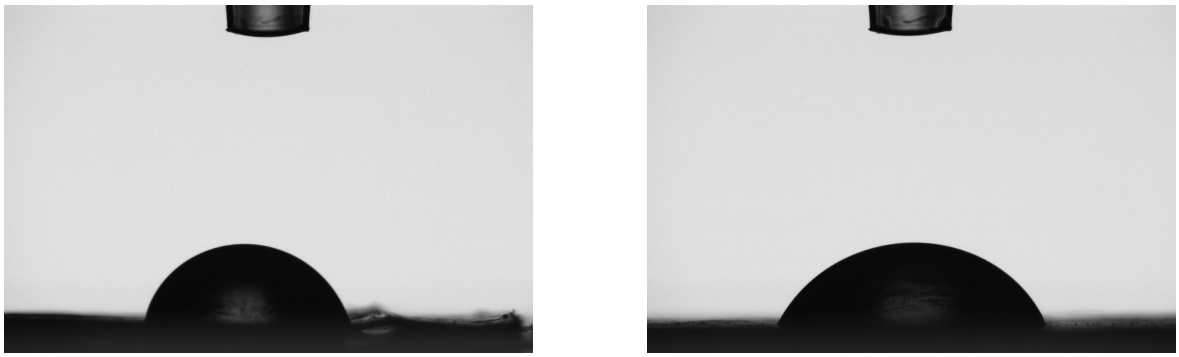

a *b*

Fig. 6. Wetting PAN (*a*) and PAN-HZD (*b*) with water

Indeed, modifying membranes with HZD results in a decrease of water wetting angle (Fig. 6). The strongest effect was found for the PA-based materials: it is caused by carboxyl groups as well as by incorporated particles of the inorganic ion-exchanger. The enhancement of PVDF hydrophilicity is due to HZD. In the case of ultrafiltration PAN membrane, its hydrophilicity is improved by incorporated inorganic particles as well as by amino- and carboxyl surface groups.

Filtration of water and calibrating solution. Besides the improvement of rejection ability and stability against fouling, the inorganic ion exchanger provides stability of the membranes against compression similarly to rigid polymer

[94]. As an example, Fig. 7 illustrates a dependence of the volume of filtrated water on time. First the $V-\tau$ curves are not linear due to compression, then they become linear. For microfiltration membranes, the time to achieve a steady state is 40 (pristine membrane) and 20 min (modified materials). Both pristine and modified ultrafiltration membranes are stable against compression.

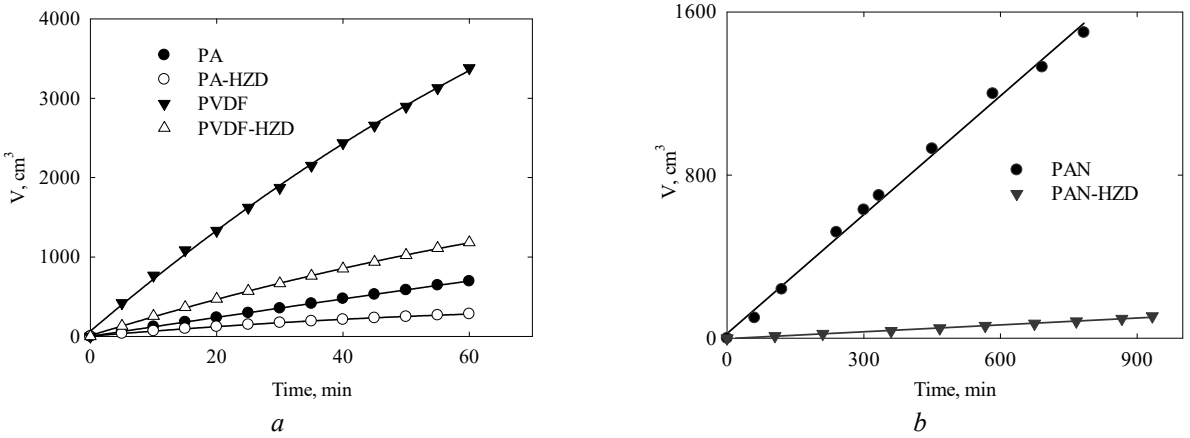

Fig. 7. Cumulative water volume through polymer and polymer-inorganic micro- (*a*) and ultrafiltration (*b*) membranes as a function of time. Pressure: 1 (*a*) and 2 (*b*) bar

Both pristine and modified membranes obey Darcy law at least up to 2 bar (Fig. 8). In other words, the water flux is proportional to pressure (ΔP):

$$J_w = \frac{\Delta P}{\mu R_m}, \qquad (6)$$

where μ is the dynamic viscosity, R_m is the hydrodynamic resistance of membranes. As follows from Table 2, the resistance decreases within the order: PVDF > PA > PAN for pristine samples. The same order was obtained for the modified membranes. Incorporated HZD increases hydrodynamic resistance approximately in 2–3 (microfiltration membranes) and 16 (ultrafiltration membranes) times.

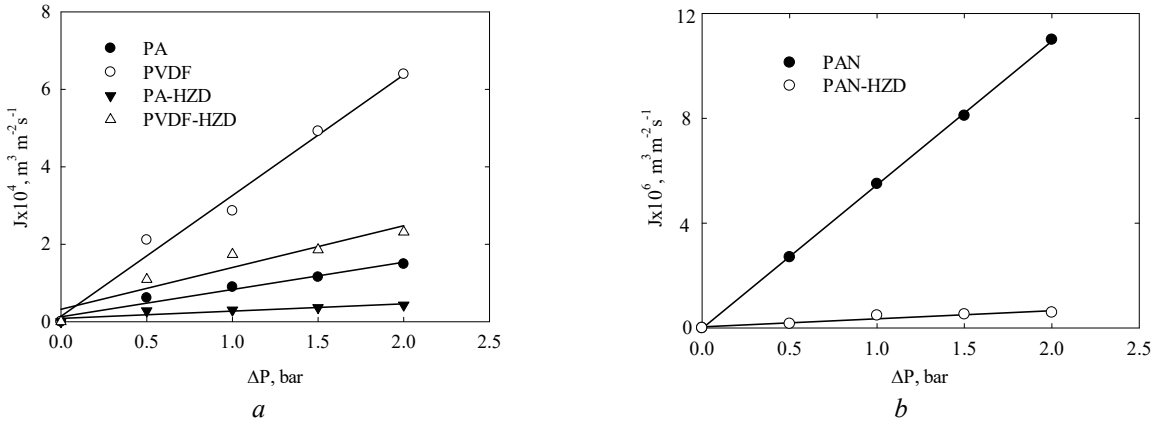

Fig. 8. Water flux through polymer and polymer-inorganic micro- (*a*) and ultrafiltration (*b*) membranes as a function of pressure

For filtration membranes, following phenomenological equation is valid [84]:

$$J = L\Delta P, \qquad (7)$$

where L is the membrane permeability (phenomenological coefficient) that is traditionally expressed in units of l m^{-2} $h^{-1}$$bar^{-1}$.

The order of the permeability decrease is: PVDF> PVDF-HZD> PA> PA-HZD> PAN> PAN-HZD. It means, even the modified PVDF sample shows the highest permeability coefficient among the modified samples as well as pristine PA and PAN membranes.

The membrane permeability is determined by porosity (ε), namely by the ratio of the volumes of pores (V_p) and membrane (V_m):

$$\varepsilon = \frac{V_p}{V_m}, \tag{8}$$

On the other hand, the permeability depends on the pore size (d), which can be calculated from the Hagen-Poiseuille equation [84]:

$$d = 2\sqrt{\frac{8\mu t \Delta x J}{\varepsilon \Delta P}}, \tag{9}$$

where t is the tortuosity coefficient (as a rule, it is close to 2 [95]), Δx is the membrane thickness. The ε and d values are given in Table 2. It should be noted that the porosity decreases after modifying due to HZD insertion (all membranes) or gluing polymer regions (PA, PAN). The d magnitude also decreases.

For asymmetric membranes, this parameter is approximate, since the porosity of active layer and macroporous support cannot be divided. However, it allows us to recognize a change of morphology. HZD particles can be located either only in the macroporous support (when large particles are formed) or in the active layer and support. The inorganic filler in the support cannot affect separation properties of the membrane. However, the modifier can influence the rejection ability, when it is placed in the active layer. Based on the energy dispersive spectra (a presence of Zr on the membrane surface), it is possible to expect the modifying effect on separation. When the BSA solution passed through the membranes, lower permeate flux was recorded in comparison with water filtration. As seen from Table 2, the *FDR* parameter was 81–93 % (microfiltration membranes) and 44–64 % (ultrafiltration membrane). It means that the PAN-based samples shows higher stability against fouling. Also the modifying procedure results in a decrease of the *FDR* value. The filtration rate reduces over time (pristine membranes) and remains practically constant in the case of modified membranes (Fig. 9).

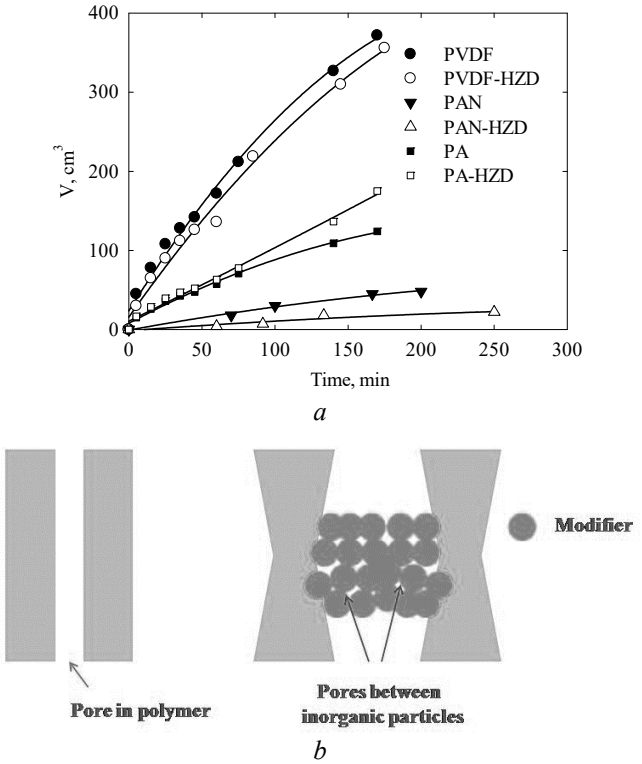

Fig. 9. Cumulative volume of permeate over time of BSA filtration (*a*), stretching of pores with HZD (*b*)

After modifying, microfiltration membranes are capable to reject BSA – the selectivity reaches 90–96 % as opposed to pristine samples, which show no selectivity. However, the modifying procedure causes an appearance of large pores in the active layers (see Fig. 2). This can be explained by stretching pores due to incorporated particles (see Fig. 8). Pores between HZD particles determine selectivity of the modified membranes. The embedded particles are stable against pressure at least at $\Delta P \leq 2$ bar evidently due to the polymer elasticity. On the other hand, the transformation of PA and PAN due to hydrolysis enhances the fixation of HZD particles in the polymers. Thus, both water and BSA tests show a positive effect of the modifier on the separation ability of membranes.

Recovery of QPE from water. QPE in water is emulsion, drops of which can demonstrate coalesce under the influence of pressure [96]. Other factors that promote coalescence are membrane material, pore size and so on. Namely the coalescence phenomenon provides rejection of this pesticide. Additionally QPE can be retained by the membrane due to adsorption. on the outer surface and/or inside pores.

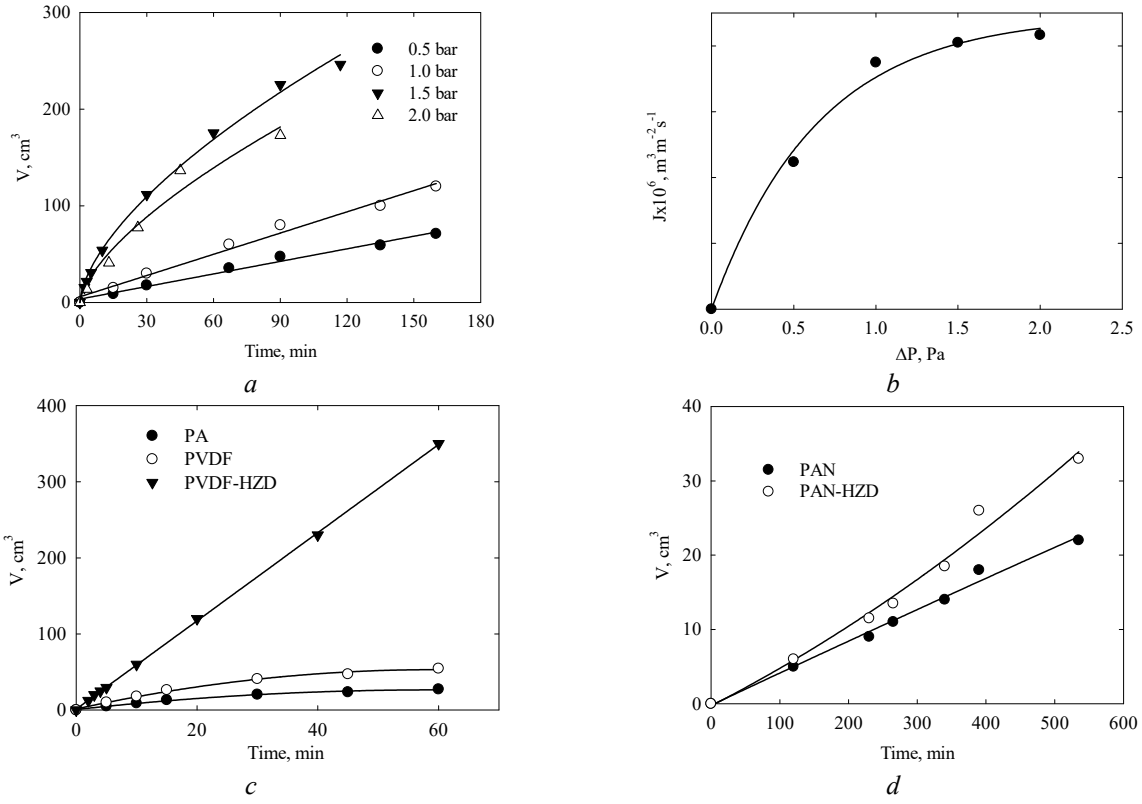

Fig. 10. Cumulative volume of permeate over time of QPE filtration through the PA-HZD sample under various pressure (*a*), permeate flux through the PA-HZD as a function of pressure (*b*), cumulative volume of permeate over time through micro- (*c*) and ultrafiltration (*d*) membranes at 1 bar

As an example, Fig. 10 *a* illustrates the effect of pressure on the liquid transport through the PA-HZD membrane. An increase of pressure from 0.5 to 1 bar enhances the transport, the V–τ dependencies are linear indicating no effect of fouling on the filtration rate. The increase in pressure up to 1.5 bar allows us to obtain the highest volume of the permeate, however, filtration slows down over time. A smaller volume of permeate was found at 2 bar than that for 1.5 bar. The dependence of the permeate flux on pressure shows a region of rapid increase followed by a plateau. The growth corresponds to the "Darcy region", the plateau is attributed to the diffusion regime. Thus, other membranes were tested at 1 bar.

According to Fig. 10 and Table 2, modified membranes show higher filtration rate of QPE-containing solution comparing with pristine material. This is opposed to the BSA filtration

indicating more intensive fouling of the pristine membrane with pesticide. Indeed, the *FDR* parameter for the pesticide filtration through the pristine material is higher than that for the BSA solution. Conversely, lower *FDR* values were found for the modified membranes in the case of QPE filtration comparing with BSA.

This behaviour of pristine and composite membranes is explained by different mechanisms of their fouling. As an example, the data for PA and PA-HZD samples were considered. Regarding to the modified membrane, the $V-\tau$ dependence obtained at 1.5 bar was analyzed, since it shows the fouling effect. Linearity of the $\tau/V-\tau$ plot indicates pore constriction, the linear $\tau/V-V$ curve means cake formation. Fig. 11 shows pore constriction for the pristine membrane and cake formation for the modified sample.

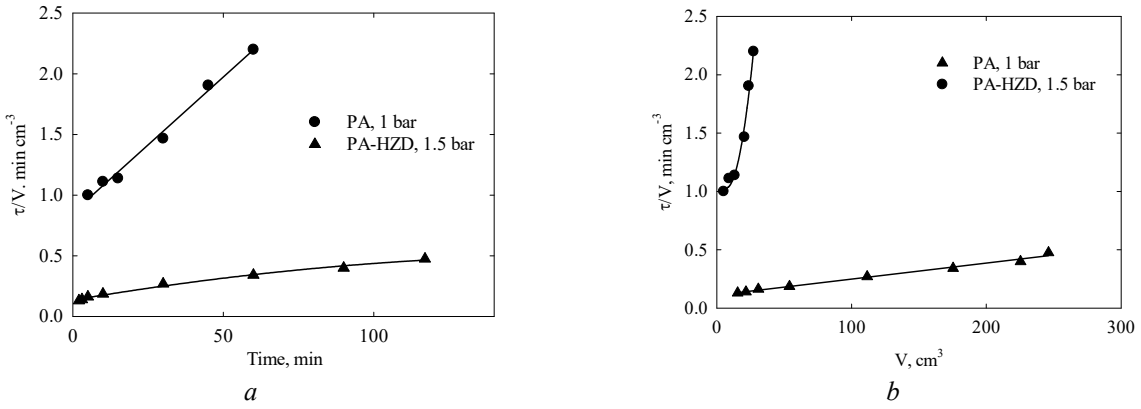

Fig. 11. Modelling of fouling: pore constriction (*a*) and cake formation (*b*)

The initial concentration of QPE was 59 mg l^{-1}, the maximal allowable concentration is 0.0001 mg l^{-1} [98]. The pesticide content in permeate decreases in 7000–300000 times, it means the membrane selectivity exceeds 99 % in all cases. An order of the QPE removal is as follows: PVDF < PVDF-HZD < PA < PA-HZD < PAN < PAN-HZD. In other words, ultrafiltration membranes demonstrate higher rejection comparing with microfiltration samples. Among microfiltration membranes, the highest retention was found for PA-based materials. In all cases, modified membranes show higher QPE rejection. The highest ratio of the volumes of permeate (V) and feeding solution (V_f) was obtained for the PVDF-HZD membrane (see Table 2). In this case, the most concentrated solution is formed.

It should be stressed that any membrane does not reduce the QPE content down to the maximal allowable concentration for surface water (0.0001 mg l^{-1}) [98]. Thus, a posttreatment of the permeate is necessary. Adsorption on biochar under dynamic conditions gives a possibility to reduce the pesticide amount down to the value, which is lower than the maximal allowable concentration: 0.00001 (PA), 0.00004 (PVDF), 0.00002 (PVDF-HZD) mg l^{-1}. Regarding to the permeate obtained with other membranes, no QPE was detected after the passage through the adsorption column. It means that the concentration is below the detection limit of the liquid chromatography method.

Since the posttreatment procedure is needed in all cases, the PVDF-HZD membrane looks most attractive. Namely this membrane produces the largest amount of permeate, the concentrate solution contains 180 mg l^{-1} QPE. This is a commercial product. According to the data of producing company, the consumption of the solution containing 125 g l^{-1} QPE is ≈ 1 liter per one hectare. The concentrate consumption is about 0.7 l per 10 m^2. This product can be recommended to prevent grass growth between paving slabs, on the cemetery plots, small lawns and so on.

CONCLUSIONS

In comparison with polymer membranes, polymer-inorganic materials containing HZD possess a number of advantages: (i) enhanced separation ability, (ii) stability against fouling with organic substances, (iii) operating under low pressure, (iii) enhanced stability against

compression, which gives a possibility to use polymer-inorganic materials for the production of hollow-fiber and capillary modules. The membranes demonstrate high QPE rejection evidently due to coalescence of the emulsion drops. Among investigated membranes, the PVDF-HZD sample shows the highest permeate flux. The concentrate solution can be used as a commercial product, the posttreatment procedure must be applied to the permeate in order to reduce an amount of toxic substance down to the maximal allowable concentration. This procedure can be not only adsorption, but also photocatalytic or chemical oxidation with ozone or Fenton reagent. These approaches would provide not only the pesticide degradation, but also the destruction of other components of the commercial form of pesticide, such as dyes, stabilizers, residual solvents.

Полімер-неорганічні мембрани для видалення пестицидів з води із використанням баромембранного методу

Ю.С. Дзязько, Л.М. Рождественська, К.О. Куделко, Л.М. Пономарьова, Л.Я. Штейнберг, Т.В. Яценко

Інститут загальної та неорганічної хімії ім. В.І. Вернадського Національної Академії Наук України
просп. Академіка Палладіна, 32/34, Київ, 03142, Україна, dzyazko@gmail.com
Сумський державний університет
вул. Харківська, 116, Суми, 40000, Україна
Науково-технічна установа "Інститут хімічної технології та промислової екології"
пл. Хіміків, 3, Рубіжне, 93000, Україна

Пестициди потрапляють до поверхневих та підземних вод не лише зі сільськогосподарських угідь, а й із підприємств. де виробляють та фасують ці речовини. Таким чином, необхідно вирішити проблему стічних вод цих підприємств. Дану роботу присвячено розробці високоефективних матеріалів для баромембранних процесів, які б були спрямовані на видалення пестицидів з води із подальшим використанням концентрату. Поліамідні (ПА) та полівініліденфторидні (ПВДФ) мікрофільтраційні мембрани, а також поліакрилонітрильні (ПАН) ультрафільтраційні мембрани модифікували гідратованим діоксидом цирконію (ГДЦ) шляхом осадження іоніту із золю парами амоніаку безпосередньо в порах полімеру. Мембрани досліджували методом СЕМ, також використовували енергодисперсійну рентгенівську та ІЧ-Фур'є спектроскопію. ГДЦ в активному шарі, а також продукти гідролізу ПА або ПАН підвищують гідрофільність поверхні мембрани: наприклад, контактний кут води зменшується з 69° до 43° для зразка ПА. Для тестування мембран використовували воду як робочу рідину. Розрахунки за рівнянням Хагена-Пуазейля показали зменшення розміру пор модифікованих мембран у ≈2–3 рази порівняно з немодифікованими. Селективність ГДЦ-вмісних мембран досягає 90–96 % відносно бичачого сироваткового альбуміну та перевищує 99 % у випадку хізалофоп-п-етилу. Найбільше значення потоку пермеату (196 л м$^{-2}$ год$^{-1}$ атм$^{-1}$) було виявлено для зразка ПВДФ, що містить ГДЦ. Концентрація пестициду у пермеаті становила 0.0002–0.008 мг л$^{-1}$. Додаткова обробка пермеату включала адсорбцію на біовугіллі в динамічних умовах. Згідно даних методу рідинної хроматографії, така обробка дозволяє зменшити вміст пестициду в розчині до рівня, нижчого за межу визначення або гранично припустиму концентрацію для поверхневих вод (0.0001 мг л$^{-1}$).

***Ключові слова**: ультрафільтрація, мікрофільтрація, пестицид, гідратований діоксид цирконію, адсорбція*

REFERENCES

1. Pisharody L., Gopinath A., Malhotra M., Nidheesh P.V., Kumar M.S. Occurrence of organic micropollutants in municipal landfill leachate and its effective treatment by advanced oxidation processes. *Chemosphere* 2022. **287**(Part 2): 132216.
2. Reberski J.L., Terzic J., Maurice L.D., Lapworth D.J. Emerging organic contaminants in karst groundwater: a global level assessment. *J. Hydrol*. 2022. **604**: 127242.
3. Halbach K., Moder M., Schrader S., Liebmann L., Schafer R.B., Schneeweiss A., Schreiner V.C., Vormeier P., Weisner O., Liess M., Reemtsma T. Small streams–large concentrations? Pesticide monitoring in small agricultural streams in Germany during dry weather and rainfall. *Water Res*. 2021. **203**: 117535.
4. Zhou Y., Meng J., Zhang M., Chen S., He B., Zhao H., Li Q., Zhang S., Wang T. Which type of pollutants need to be controlled with priority in wastewater treatment plants: traditional or emerging pollutants? *Environ. Int.* 2019. **131**: 104982.
5. Syafrudin M., Kristanti R.A., Yuniarto A., Hadibarata T., Rhee J., Al-onazi W.A., Algarni T.S., Almarri A.H., Al-Mohaimeed A.M. Pesticides in drinking water – a review. *Int. J. Environ. Res. Public Health*. 2021. **18**(2): 468.
6. Szocs E., Brinke M., Karaoglan B., Schafer R.B. Large Scale Risks from Agricultural Pesticides in Small Streams. *Environ. Sci. Technol.* 2017. **51**(13): 7378.
7. Zhang Ye., Li J.-N., Wang J.-X., Li Y.F., Kallenborn R., Xiao H., Cai M.-G., Tang Z.-H., Zhang Z.-F. High-throughput screening of 222 pesticides in road environments in a megacity of northern China: A new approach to urban population exposure. *Environ. Res*. 2024. **257**: 119379.
8. Choudri B.S., Charabi Y., Al-Nasiri N., Al-Awadhi T. Pesticides and herbicides. *Water Environ. Res*. 2020. **92**: 1425.
9. Cui S., Hough R., Yates K., Osprey M., Kerr C., Cooper P., Coull M., Zhang Z. Effects of season and sediment-water exchange processes on the partitioning of pesticides in the catchment environment: implications for pesticides monitoring. *Sci. Total Environ*. 2020. **698**: 134228.
10. Gramlich A., Stoll S., Stamm C., Walter T., Prasuhn V. Effects of artificial land drainage on hydrology, nutrient and pesticide fluxes from agricultural fields – a review. *Agric. Ecosyst. Environ*. 2018. **266**: 84.
11. Vryzas Z. Pesticide fate in soil-sediment-water environment in relation to contamination preventing actions. *Curr. Opin. Environ. Sci. Health*. 2018. **4**: 5.
12. Mello M.F., Scapini R. Reverse logistics of agrochemical pesticide packaging and the impacts to the environment. *Braz. J. Operat. Product. Manag*. 2016. **13**: 110.
13. Garbounis G., Karasali H., Komilis D. A life cycle analysis to optimally manage wasted plastic pesticide containers. *Sustainability.* 2022. **14**(14): 8405.
14. Mohafrash S.M., Mossa A.T.H. Disposal of expired empty containers and waste from pesticides. *Egypt. J. Chem*. 2024. **67**(4): 65.
15. Yuan S., Arellano A.F., Knickrehm L., Chang H., Christopher L., Castro C.L., Furlong M. Towards quantifying atmospheric dispersion of pesticide spray drift in Yuma County Arizona. *Atmos. Environ.* 2024. **319**: 120262.
16. Oldenkamp R., Benestad R.E., Hader J.D., Mentzel S., Nathan R., Madsen A.L., Moe S.J. Incorporating climate projections in the environmental risk assessment of pesticides in aquatic ecosystems. *Integr. Environ. Assess. Manage.* 2024. **20**(2): 384.
17. Bighiu M.A., Höss S., Traunspurger W., Kahlert M., Goedkoop W. Limited effects of pesticides on stream macroinvertebrates, biofilm nematodes, and algae in intensive agricultural landscapes in Sweden. *Water Res*. 2024. **174**: 115640.
18. Sumudumali R.G.I., Jayawardana J. A review of biological monitoring of aquatic ecosystems approaches: with special reference to macroinvertebrates and pesticide pollution. *Environ. Manage.* 2021. **67**: 263.
19. Rohani M.F. Pesticides toxicity in fish: Histopathological and hemato-biochemical aspects – A review. *Emerging Contam*. 2023. **9**(3):100234.
20. Syafrudin M., Kristanti R.A., Yuniarto A., Hadibarata T., Rhee J., Al-onazi W.A., Algarni T.S., Almarri A.H., Al-Mohaimeed A.M. Pesticides in Drinking Water – A Review. *Int. J. Environ. Res. Public Health*. 2021. **18**(2): 468.
21. Kamata M., Matsui Y., Asami M. National trends in pesticides in drinking water and water sources in Japan. *Sci. Total Environ*. 2020. **744**: 140930.
22. Wang D., Yu Y., Zhang X., Zhang D., Zhang S., Wu M. Organochlorine pesticides in fish from Taihu Lake, China, and associated human health risk assessment. *Ecotoxicol. Environ. Safety*. 2013. **98**: 383.
23. Abbassy M.A., Khalifa M.A., Nassar A.M.K., El-Deen E.E.N., Salim Y.M. Analysis of organochlorine pesticides residues in fish from Edko Lake (North of Egypt) using eco-friendly method and their health implications for humans. *Toxicol. Res.* 2021. **37**(4): 495.

24. Kim K.-H., Kabir E., Jahan S.A. Exposure to pesticides and the associated human health effects. *Sci. Total Environ*. 2017. **575**: 525.
25. Sabarwal A., Kumar K., Singh R.P. Hazardous effects of chemical pesticides on human health – Cancer and other associated disorders. *Environ. Toxicol. Pharmacol*. 2018. **63**: 103.
26. Saleh I.A., Zouari N., Al-Ghouti M.A. Removal of pesticides from water and wastewater: chemical, physical and biological treatment approaches. *Environ. Technol. Innovation.* 2020. **19**: 101026.
27. Cruz-Alcalde A., Sans C., Esplugas S. Priority pesticides abatement by advanced water technologies: the case of acetamiprid removal by ozonation. *Sci. Total Environ*. 2017. **599–600**: 1454.
28. Ejeta S.Y., Imae T. Photodegradation of pollutant pesticide by oxidized graphitic carbon nitride catalysts. *J. Photochem. Photobiol. Chem.* 2021. **404**: 112955.
29. Salam M.A., Abu Khadra M.R., Mohamed A.S. Effective oxidation of methyl parathion pesticide in water over recycled glass based-MCM-41 decorated by green Co_3O_4 nanoparticles. *Environ. Pollut*. 2020. **259**: 113874.
30. Farré M.J, Franch M.I., Malato S., Ayllón J.A., Peral J., Doménech X. Degradation of some biorecalcitrant pesticides by homogeneous and heterogeneous photocatalytic ozonation. *Chemosphere*. 2005. **58**(8): 1127.
31. Solís R.R., Rivas F.J., Martínez-Piernas A., Agüera A. Ozonation, photocatalysis and photocatalytic ozonation of diuron. Intermediates identification. *Chem. Eng. J.* 2016. **292**: 72.
32. Brillas E. Fenton, photo-Fenton, electro-Fenton, and their combined treatments for the removal of insecticides from waters and soils. A review. *Sep. Purif. Technol.* 2022. **284**: 120290.
33. Bano K., Kaushal S., Singh P.P. A review on photocatalytic degradation of hazardous pesticides using heterojunctions. *Polyhedron*. 2021. **209**: 115465.
34. Khan S.H., Pathak B. Zinc oxide based photocatalytic degradation of persistent pesticides: a comprehensive review. *Environ. Nanotechnol. Monit. Manage.* 2020. **13**: 100290.
35. Meephon S., Rungrotmongkol T., Puttamat S., Praserthdam S., Pavarajarn V. Heterogeneous photocatalytic degradation of diuron on zinc oxide: influence of surface-dependent adsorption on kinetics, degradation pathway, and toxicity of intermediates. *J. Environ. Sci*. 2019. **84**: 97.
36. Chiron S., Fernandez-Alba A., Rodriguez A., Garcia-Calvo E. Pesticide chemical oxidation: state-of-the-art. *Water Res*. 2000. **34**(2): 366.
37. Trellu C., Olvera Vargas H., Mousset E., Oturan N., Oturan M.A. Electrochemical technologies for the treatment of pesticides. *Curr. Opin. Electrochem*. 2021. **26**: 100677.
38. Xu J., Olvera-Vargas H., Teo F.Y.H., Lefebvre O. A comparison of visible-light photocatalysts for solar photoelectrocatalysis coupled to solar photoelectro-Fenton: application to the degradation of the pesticide simazine. *Chemosphere*. 2021. **276**: 130138.
39. Ning Y., Li K., Zhao Z., Chen D., Li Y., Liu Y., Yang Q., Jiang B. Simultaneous electrochemical degradation of organophosphorus pesticides and recovery of phosphorus: synergistic effect of anodic oxidation and cathodic precipitation. *J. Taiwan Inst. Chem. Eng*. 2021. **125**: 267.
40. Raschitor A., Llanos J., Cañizares P., Rodrigo M.A. Novel integrated electrodialysis/electro-oxidation process for the efficient degradation of 2, 4-dichlorophenoxyacetic acid. *Chemosphere*. 2017. **182**: 85.
41. Ryan D.R., Maher E.K., Heffron J., Mayer B.K., McNamaran P.J. Electrocoagulation-electrooxidation for mitigating trace organic compounds in model drinking water sources. *Chemosphere*. 2021. **273**: 129377.
42. Raschitor A., Llanos J., Rodrigo M.A., Cañizares P. Combined electrochemical processes for the efficient degradation of non-polar organochlorine pesticides. *J. Environ. Manage*. 2019. **248**: 109289.
43. Ghalwa M.A.N., Farhat B.N. Removal of imidacloprid pesticide by electrocoagulation process using iron and aluminum electrodes. *J. Environ. Anal. Chem*. 2015. **2**(4): 1000154.
44. Babu B.R., Meera K.M.S., Venkatesan P. Removal of pesticides from wastewater by electrochemical methods A comparative approach. *Sustain. Environ. Res*. 2011. **21**(6): 401.
45. Alfredy T., Elisadiki J., Jande Y.A.C. Capacitive deionization for the removal of paraquat herbicide from aqueous solution. *Adsorption Sci. Technol*. 2021. **2021**(149): 1.
46. Monga D., Kaur P., Singh B. Microbe mediated remediation of dyes, explosive waste and polyaromatic hydrocarbons, pesticides and pharmaceuticals. *Curr. Res. Microb. Sci*. 2022. **3**: 100092.
47. Bose S., Kumar P.S., Vo D.-V.N., A review on the microbial degradation of chlorpyrifos and its metabolite TCP. *Chemosphere.* 2021. **283**: 131447.
48. Tarla D.N., Erickson L.E., Hettiarachchi G.M., Amadi S.I., Galkaduwa M., Davis L.C., Nurzhanova A., Pidlisnyuk V. Phytoremediation and bioremediation of pesticide-contaminated soil. *Appl. Sci*. 2020. **10**: 1217.
49. Pedroso M.M., Hine D., Hahn S., Chmielewicz W.M., Diegel J., Gahan L., Schenk G. Pesticide degradation by immobilised metalloenzymes provides an attractive avenue for bioremediation. *EFB Bioecon. J.* 2021. **1**: 100015.

50. Mahlalela L.C., Casado C., Marugan J., Septien S., Ndlovu T., Dlamini L.N. Coupling biological and photocatalytic treatment of atrazine and tebuthiuron in aqueous solution. *J. Water Process. Eng*. 2021. **40**: 101918.
51. Zhang Y., Cao X., Yang Y., Guan S., Wang X., Li H., Zheng X., Zhou L., Jiang Y., Gao J. Visible light assisted enzyme-photocatalytic cascade degradation of organophosphorus pesticides. *Green Chem. Eng*. 2023. **4**(1): 30.
52. Sarker A., Nandi R., Kim J.-E., Islam T. Remediation of chemical pesticides from contaminated sites through potential microorganisms and their functional enzymes: prospects and challenges. *Environ. Technol. Innovation*. 2021. **23**: 101777.
53. Wang Y., Lin C., Liu X., Ren W., Huang X., He M., Ouyang W. Efficient removal of acetochlor pesticide from water using magnetic activated carbon: Adsorption performance, mechanism, and regeneration exploration. *Sci. Total Environ*. 2021. **778**: 146353.
54. Dzyazko Yu.S., Palchik O.V., Ogenko V.M., Shtemberg L.Ya., Bogomaz V.I., Protsenko S.A., Khomenko V.G., Makeeva I.S., Chernysh O.V., Dzyazko O.G. Nanoporous biochar for removal of toxic organic compounds from water. *Springer Proceedings in Physics*. 2019. **222**: 209.
55. Nassar A.E., El-Aswar E.I., Rizk S.A., El-Sayed Gaber S., Jahin H.S. Microwave-assisted hydrothermal preparation of magnetic hydrochar for the removal of organophosphorus insecticides from aqueous solutions. *Sep. Purif. Technol*. 2023. **306**(A): 122569.
56. Masini J.C., Abate G. Guidelines to study the adsorption of pesticides onto clay minerals aiming at a straightforward evaluation of their removal performance. *Minerals.* 2021. **11**(11): 1282.
57. Andrunik M., Bajda T. Removal of pesticides from waters by adsorption: comparison between synthetic zeolites and mesoporous silica materials. A review. *Materials.* 2021. **14**(13): 3532.
58. Dinu I.A., Ghimici L., Raschip I.E. Macroporous 3D chitosan cryogels for Fastac 10EC pesticide adsorption and antibacterial applications. *Polymers.* 2022. **14**(15): 3145.
59. Mehmeti V., Halili J., Berisha A. Which is better for Lindane pesticide adsorption, graphene or graphene oxide? An experimental and DFT study. *J. Mol. Liq*. 2022. **347**: 118345.
60. Dzyazko Yu.S., Ogenko V.M., Shteinberg L.Ya., Bildyukevich A.V., Yatsenko T.V. Composite adsorbents including oxidized graphene: effect of composition on mechanical durability and adsorption of pesticides. *Him. Fiz. Tehnol. Poverhni*. 2019. **10**(4): 432.
61. Tang J., Ma X., Yang J., Feng D.D., Wang X.Q. Recent advances in metal–organic frameworks for pesticide detection and adsorption. *Dalton Trans*. 2020. **49**(43): 14361.
62. Qi P., Wang J., Li H., Wu Y., Liu Z., Zheng B., Wang X. Fluffy ball-like magnetic covalent organic frameworks for adsorption and removal of organothiophosphate pesticides. *Sci. Total Environ*. 2022. **840**: 156529.
63. Costa F.C.R., dos Santos C.R., Amaral M.C.S. Trace organic contaminants removal by membrane distillation: A review on mechanisms, performance, applications, and challenges. *Chem. Eng. J*. 2023. **464**: 142461.
64. Musbah I., Ciceron D., Saboni A., Alexandrova S. Removal of pesticides and desethylatrazine (DEA) by nanofiltration: effects of organic and inorganic solutes on solute rejection. *J. Chem. Technol. Metall*. 2018. **53**(4): 657.
65. Fujioka T., Kodamatani H., Yujue W., Yu K.D., Wanjaya E.R., Yuan H., Fang M., Snyder S.A. Assessing the passage of small pesticides through reverse osmosis membranes. *J. Membr. Sci.* 2020. **595**: 117577.
66. Zheng L., Price W.E., McDonald J., Khan S.J., Fujioka T., Nghiem L.D. New insights into the relationship between draw solution chemistry and trace organic rejection by forward osmosis. *J. Membr. Sci*. 2019. **587**: 117184.
67. Zhang Y., Lu H., Wang B., Zhang Z., Lin X., Chen Z., Li B. Removal of imidacloprid and acetamiprid from tea infusions by microfiltration membrane. *Int. J. Food Sci. Technol*. 2015. **50**(6): 1397.
68. Jolivalt C., Brenon S., Caminade E., Mougin C., Pontié M. Immobilization of laccase from *Trametes versicolor* on a modified PVDF microfiltration membrane: characterization of the grafted support and application in removing a phenylurea pesticide in wastewater. *J. Membr. Sci*. 2000. **180**(1): 103.
69. Doulia D.S., Anagnos E.K., Liapis K.S., Klimentzos D.A. Removal of pesticides from white and red wines by microfiltration. *J. Hazard. Mater*. 2016. **317**: 135.
70. Zmievskii Y., Rozhdestvenska L., Dzyazko Y., Kornienko L., Myronchuk V., Bildyukevich A., Ukrainetz A. Organic-inorganic materials for baromembrane separation. *Springer Proc. Phys*. 2017. **195**: 675.
71. Dzyazko Y.S., Rozhdestvenskaya L.M., Zmievskii Y.G., Vilenskii A.I., Myronchuk V.G., Kornienko L.V., Vasilyuk S.V., Tsyba N.N. Organic-inorganic materials containing nanoparticles of zirconium hydrophosphate for baromembrane separation. *Nanoscale Res. Lett*. 2015. **10**: 64.
72. Rozhdestvenska L., Kudelko K., Ogenko V., Palchik O., Plisko T., Bildyukevich A., Zakharov V., Zmievskii Yu., Vishnevskii O. Filtration membranes containing nanoparticles of hydrated zirconium oxide – graphene oxide. 2020. *Springer Proc. Phys*. **246**: 757.

73. Dzyazko Y., Rozhdestvenska L., Kudelko K., Ogenko V., Kolomiets Y. Membranes modified with advanced carbon nanomaterials (review*). Springer Proc. Phys*. 2021. **263**: 151.
74. Rozhdestvenska L., Kudelko K., Ogenko V., Bildyukevich A., Plisko T., Borisenko Yu., Chmilenko V. Membranes modified by nanocomposites of hydrated zirconium dioxide and oxidized graphene*. Ukr. Chem. J.* 2020. **86**(4): 91.
75. Kudelko K., Rozhdestvenskaya L., Ogenko V., Chmilenko V. Formation and characterization of porous anodized aluminum oxide, synthesized electrochemically in the presence of graphene oxide. *Appl. Nanosci*. 2022. **12**: 1967.
76. Kudelko K.O., Rozhdestvenska L.M., Ponomarova L.M., Ogenko V.M. Anodic aluminum oxide-membrane prepared in electrolyte “oxalic acid – matter with carbon nanodots”. *Him. Fiz. Tehnol. Poverhni*. 2023. **14**(2): 237.
77. Maltseva T.V., Kolomiets E.O., Dzyazko Yu.S., Scherbakov S. Composite anion-exchangers modified with nanoparticles of hydrated oxides of multivalent metals. *Appl. Nanosci*. 2019. **9**(5): 997.
78. Bildyukevich A.V., Plisko T.V., Shustikov A.A., Dzyazko Yu.S., Rozhdestvenska L.M., Pratsenko S.A. Effect of the solvent nature on the structure and performance of poly(amide-imide) ultrafiltration membranes. *J. Mater. Sci*. 2020. **55**(22): 9638.
79. Perlova O.V., Dzyazko Yu.S., Palchik A.V., Ivanova I.S., Perlova N.O., Danilov M.O., Rusetskii I.A., Kolbasov G.Ya., Dzyazko A.G. Composites based on zirconium dioxide and zirconium hydrophosphate containing graphene-like additions for removal of U(VI) compounds from water. *Appl. Nanosci*. 2020. **10**: 4591.
80. Dzyazko Yu., Volfkovich Yu., Perlova O., Ponomaryova L., Perlova N., Kolomiets E. Effect of porosity on ion transport through polymers and polymer-based composites containing inorganic nanoparticles (review). *Springer Proc. Phys*. 2019. **222**: 235.
81. Kudelko K., Maltseva T., Bieliakov V. Adsorption and mobility of Cu (II), Cd (II), Pb (II) ions adsorbed on (hydr)oxide polymer sorbents M_xO_y•nH_2O, M = Zr (IV), Ti (IV), Sn (IV), Mn (IV). *Desalin. Water Treat.* 2011. **35**(1–3): 295.
82. Mal’tseva T.V., Yatsenko T.V., Kudelko E.O., Belyakov V.N. The effect of introduction of manganese hydroxide and hydrated aluminum oxide on the pore structure and surface charge of Zr(IV), Ti(IV), and Sn(IV) oxyhydrates. *Russ. J. Appl. Chem*. 2011. **84**(5): 726.
83. Kudelko E., Mal’tseva T., Belyakov V. Sorption of Cr(VI) ions by oxyhydrates of M_x $Al_{1-x}O_y \cdot nH_2O$ composition, where M is Zr(IV), Ti(IV), or Sn(IV). *Colloid. J.* 2012. **74**(3): 313.
84. Mulder M. *Basic Principles of Membrane Technology*. (Dordrecht, Boston, London: Kluwer Academic Publisher, 1996).
85. Bradford M.M. A rapid and sensitive method for the quantitation of microgram quantities of protein utilizing the principle of protein-dye binding. *Anal. Biochem*. 1976. **72**(1–2): 248.
86. Gao H., Zhong S., Dangayach R., Chen Y. Understanding and designing a high-performance ultrafiltration membrane using machine learning, *Environ. Sci. Technol*. 2023. **57**(46): 17831.
87. Krentsel L.B., Kudryavtsev Y.V., Rebrov A.I., Litmanovich A.D., Plate N.A. Acidic Hydrolysis of Polyacrylonitrile: Effect of Neighboring Groups. *Macromolecules.* 2001. **34**(16): 5607.
88. Kudryavtsev Y.V., Krentsel L.B., Bondarenko G.N., Litmanovich A.D., Plate N.A., Schapowalow S., Sackmann G. Alkaline hydrolysis of polyacrylonitrile, 2a. On the product swelling. *Macromol. Chem. Phys*. 2000. **201**(16): 1419.
89. Lee J.Y., Kim K.-J. MEG effects on hydrolysis of polyamide 66/glass fiber composites and mechanical property changes. *Molecules.* 2019. **24**(4): 755.
90. Nakanishi K. *Infrared Absorption Spectroscopy*. (San-Francisco, Nancodo, Tokio: Holden Day, 1962).
91. Jun B.M., Lee H.K., Kwon Y.N. Acid-catalyzed hydrolysis of semi-aromatic polyamide NF membrane and its application to water softening and antibiotics enrichment. *Chem. Eng. J*. 2018. **332**: 419.
92. Puhan M.R., Sutariya B., Karan S. Revisiting the alkali hydrolysis of polyamide nanofiltration membranes. *J. Membr. Sci*. 2022. **661**: 120887.
93. Cheraghali R., Maghsoud Z. Enhanced modification technique for polyacrylonitrile UF membranes by direct hydrolysis in the immersion bath. *J. Appl. Polym. Sci*. 2020. **137**(16): 48583.
94. Molina L.C.A., Magalhães-Ghiotto G.A.V., Nichi L., Dzyazko Y.S., Bergamasco R. Membranes modified with rigid polymer for processing solutions of vegetable proteins, *Acta Periodica Technologica*. 2023. **2023**(54): 313.
95. Manickam S.S., Gelb J., McCutcheon J.R. Pore structure characterization of asymmetric membranes: non-destructive characterization of porosity and tortuosity. *J. Membr. Sci*. 2014. **454**: 549.
96. Hong A., Fane A.G., Burford R. Factors affecting membrane coalescence of stable oil-in-water emulsions. *J. Membr. Sci*. 2003. **222**(1–2): 19.

97. Ho C.-C., Zydney A.L. A combined pore blockage and cake filtration model for protein fouling during microfiltration. *J. Colloid Interface Sci*. 2000. **232**(2): 389.
98. On the approval of the State medical and sanitary standards for the safe use of pesticides and agrochemicals. Ministry of health protection of Ukraine, order 02.02.2016, N 55, https://zakon.rada.gov.ua/laws/show/z0207-16#Text

Received 22.07.2024, accepted 25.11.2024